Structure Evolution in Amylopectin/Ethylene Glycol Mixtures by H-bond Formation and Phase Separation Studied with Dielectric Relaxation Spectroscopy

A. L. M. Smits,*,† M. Wübbenhorst,‡ P. H. Kruiskamp,† J. J. G. van Soest,§ J. F. G. Vliegenthart,† and J. van Turnhout‡

Bijvoet Center for Biomolecular Research, Utrecht University, Faculty of Chemistry, P.O. Box 80075, 3508 TB Utrecht, The Netherlands, Department of Polymer Materials & Engineering, Faculty of Applied Sciences, Delft University of Technology, Julianalaan 136, 2628 BL Delft, The Netherlands, and Agrotechnological Research Institute ATO, P.O. Box 17, 6700 AA Wageningen, The Netherlands

Received: September 15, 2000; In Final Form: March 26, 2001

The interaction between amylopectin, a starch polysaccharide, and ethylene glycol (EG) was investigated using broad-band dielectric relaxation spectroscopy. Water-free amylopectin (AP) was mixed with 21 wt % ethylene glycol. This resulted in a continuous ethylene glycol phase, as well as a molecularly mixed AP/EG fraction. After storage at room temperature or annealing, the mixture shows dynamic properties typical of a polymer with weak intermolecular interactions, suggesting that EG binds preferentially to AP and forms intrachain H-bridges leading to increased chain stiffness and thus an increased glass transition temperature. This structure evolution is accompanied by a sharp reduction in the size of the ethylene glycol droplets to a few nanometers, as revealed by pronounced confinement effects in the α-relaxation of the dispersed EG.

Introduction

Starch is used as a natural food ingredient and is, among other carbohydrates, one of the main energy providers in the human diet. Furthermore, starch-based polymeric materials are playing an increasing role as biodegradable material, which can easily be processed by molding techniques widely used for synthetic polymers. One can obtain thermoplastic starch products with a broad range of material properties, owing to the diversity of natural starch itself,[1−3] which is usually combined with a low molecular plasticizer. It is known that these properties also depend strongly on the processing conditions, such as temperature and water content. The limited knowledge about the relations between processing conditions and the resulting molecular structure and properties of starch plastics makes it difficult to predict and control their physical properties.

Ageing induced by starch retrogradation causes staling of bakery products and embrittlement of starch plastics, which deteriorate the properties of these materials.[4,5] These aging processes can be influenced in particular by plasticizers, since they strongly affect the molecular organization and hence the viscoelastic properties of the thermoplastic, semicrystalline starch plastics in time. For example, in bread the degree of retrogradation is reduced markedly by the addition of monoglycerides, which interact with amylopectin.[6] The inhibiting effect of various saccharides on retrogradation has often been reported,[7−10] and glycerol, for example, has been reported to reduce the rate of retrogradation in a waxy maize starch gel.[11]

Insight into the plasticizer−macromolecule interaction is essential for the optimization of the material properties of thermoplastic starch by controlling the molecular structure. Recently, the interactions of glycerol and ethylene glycol with dry starch polysaccharides (amylose and amylopectin) were investigated using DSC and solid-state NMR spectroscopy, showing that for both plasticizers a strong interaction is induced by heat and time.[12,13] The interaction of starch with ethylene glycol develops more rapidly than with glycerol.

Dielectric relaxation spectroscopy (DRS) has established itself as a powerful technique for the study of molecular dynamics in polymers in the past decade, ever since automated spectrometers covering a broad frequency range (10^{-3}−10^{9} Hz) became available. Although DRS is well introduced in the field of synthetic polymers, only a few dielectric studies on bioplastics have been published as yet, mainly involving carbohydrate systems. Besides the molecular assignment of dielectric relaxation processes of ionic carbohydrates, cellulose, dextran, and various starches,[14−16] changes in dielectric relaxation processes in carbohydrate systems upon addition of glycerol and water have been described.[17] Here we report on the dielectric analysis of the interaction between dry amylopectin and ethylene glycol.

Experimental Section

Dry amylopectin/ethylene glycol samples were prepared by mixing ethylene glycol (≤0.05% H_2O, Acros, B) with dried potato amylopectin (amylopectin UG, Avebe, NL). The potato amylopectin was examined with X-ray diffraction, its crystallinity being similar to that of native potato starch (∼25%). Amylopectin was dried for 48 h under reduced pressure in a vacuum oven at 70 °C. The dried material (<3% H_2O) was mixed manually under a nitrogen gas flow with 21 wt % ethylene glycol (corresponding to 4.3 mmol ethylene glycol per gram amylopectin). For the dielectric experiments disk-shaped samples were prepared by pressing the sample material between circular brass electrodes (diameter 20 mm), which resulted in 300−600 μm thick samples. Preparation took place under flowing gaseous nitrogen.

* Corresponding author.
† Bijvoet Center for Biomolecular Research.
‡ Department of Polymer Materials & Engineering.
§ Agrotechnological Research Institute ATO.

10.1021/jp003289f CCC: $20.00
Published on Web 05/26/2001

TABLE 1: Sample History and VFT Parameters of α_{EG} and α_{AP} for AP/EG Mixtures

		α_{AP}					α_{EG}		
sample	annealing temp [°C]	T_g[a] [K]	T_V [K]	E_V [kJ/mol]	log(τ_∞ [s])	m	T_V [K]	E_V [kJ/mol]	log(τ_∞ [s])
1	25	200	96.6	29.0	−12.7	28.3	131	13.5	−12.8
1	40	220	114	27.5	−11.5	28.1	110.3	25.2	−15.5
2	60	222	81.2	39.7	−12.7	23.2	133	15.4	−12.8
2	80	226	112	29.5	−11.5	26.8	74.5	36.6	−16.8
2	100	249	89	43.0	−12.0	21.8	7.3	54.5	−17.7
2	120	251	93.6	39.4	−11.1	20.9	0[b]	57.9	−18.2
3	100	224	105	30.4	−11.4	25.3	132	13.4	−12.0
3	120	249	74	45.0	−11.4	19.0	0[b]	57.1	−18.0

[a] An operationally defined T_g was derived from the VFT parameters using eq 2 with the assumption that $\tau(T_g) = 100$ s. [b] Fit with $T_V = 0$ (Arrhenius fit).

Dielectric experiments on the AP/EG mixtures were performed using a combination of two dielectric measurement systems covering a frequency range from 10^{-2} to 10^6 Hz: (1) a frequency response analyzer (Schlumberger 1260) equipped with a custom-made dielectric interface (developed by TNO) for frequencies between 10^{-2} and 10^3 Hz and (2) a Hewlett-Packard 4284A precision LCR-meter for frequencies between 10^3 and 10^6 Hz. The sample was placed in a nitrogen flushed cryostat (Novocontrol), the temperature of which was controlled with a stability of better than ±50 mK. More details about the experimental setup can be found in ref 18.

Dielectric measurements were performed on three different samples, the thermal history of which is indicated in Table 1. The temperatures given in Table 1 have the meaning of either the highest temperature (25 °C) or the temperature at which the sample was annealed just prior to a subsequent cooling run to −120 °C by steps of 5 °C. Such a cooling program was chosen to ensure that kinetic changes, if present, were restricted to the upper (start) temperature interval. The average cooling rate was about 1 °C/min.

Results and Discussion

Overview of the Relaxations and Analysis of the Dielectric Relaxation Data. A typical three-dimensional loss spectrum of sample 1, which was cooled from room temperature to −120 °C immediately after sample preparation, is shown in Figure 1. Since strong Ohmic conduction dominated the measured dielectric loss ϵ'', we have calculated the alternative loss ϵ''_{deriv} from the permittivity ϵ' according to

$$\epsilon''_{deriv} = -\frac{\pi \partial \epsilon'(\omega)}{2 \partial \ln \omega} \tag{1}$$

This yields a fair approximation of the "conduction-free" loss ϵ'' for distributed relaxation peaks like those of the α-transition and the secondary relaxations.[19,20]

By using this derivative technique, two strong and well resolved relaxation processes are revealed (cf. Figures 1 and 2), which were assigned to the dynamic glass-transitions of phase separated ethylene glycol (α_{EG})—the fast or low-temperature process—and of "plasticized" amylopectin (α_{AP}), respectively. Such α-relaxation processes can be identified by their temperature dependence of the relaxation time $\tau(T)$, which typically obeys the Vogel−Fulcher−Tammann law (eq 2), rather than the well-known Arrhenius equation:

$$\tau(T) = \tau_\infty \exp\left[\frac{E_V}{R(T-T_V)}\right] \tag{2}$$

Here the parameters R, E_V, T_V, and τ_∞ denote the gas constant,

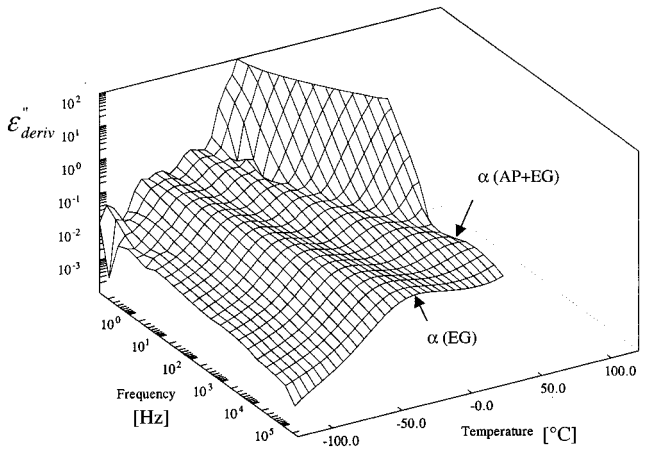

Figure 1. Three-dimensional representation of the "conduction-free" loss $\epsilon''_{deriv}(f,T)$ for a freshly mixed AP/EG sample (sample 1 in Table 1) showing two distinct non-Arrhenius α relaxation processes.

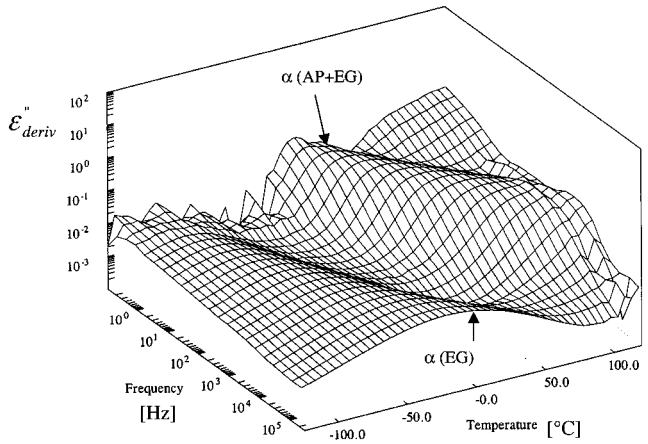

Figure 2. Three-dimensional representation of $\epsilon''_{deriv}(f,T)$ of AP/EG sample 2 after annealing at 120 °C.

the "Vogel activation energy", the "Vogel scaling temperature", and the preexponential factor.

To determine the relaxation time $\tau(T)$ from the dielectric loss curves we have fitted the loss spectra $\epsilon''(\omega)$ by a set of two Havriliak−Negami (HN) relaxation functions (eq 3), using the Levenberg−Marquardt algorithm:

$$\epsilon'' = -\sum_{k=1}^{2} \mathrm{Im}\left\{\frac{\Delta\epsilon_k}{(1+(i\omega\tau_k)^{a_k})^{b_k}}\right\} + \frac{\sigma}{\epsilon_0 \omega} \tag{3}$$

where $\Delta\epsilon_k$ and τ_k correspond to the relaxation strength and the mean relaxation time of the kth process. The two shape parameters a_k and b_k, which determine the slope $d\epsilon''/d \ln \omega$ of

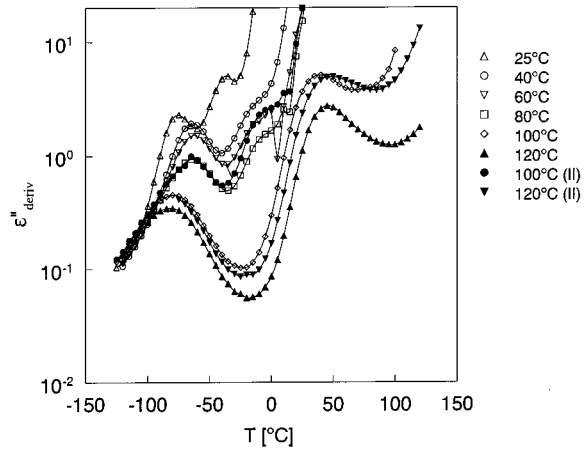

Figure 3. Temperature dependent $\epsilon''_{deriv}(f,T)$ at $f = 14$ Hz for AP/EG annealed at different temperatures.

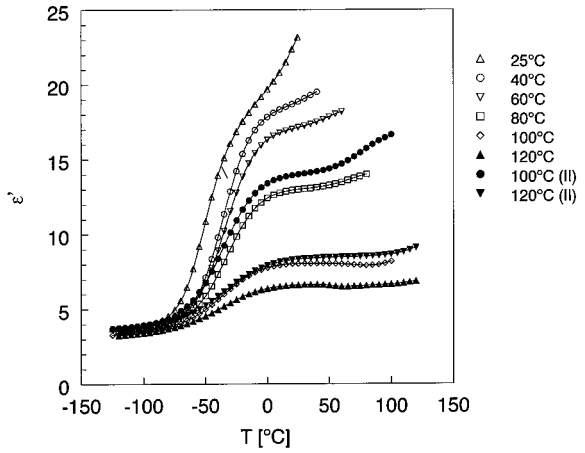

Figure 4. Temperature-dependent permittivity $\epsilon'(T)$ at $f = 28$ kHz for AP/EG annealed at different temperatures.

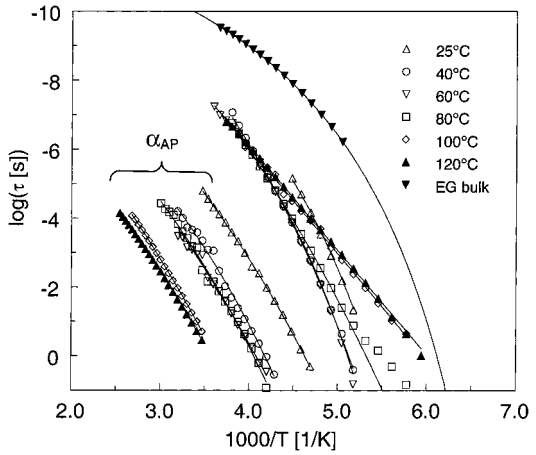

Figure 5. Relaxation map of samples 1 and 2: sample 1 fresh (25 °C), and after annealing at 40 °C, and sample 2 after annealing at 60, 80, 100, and 120 °C. For comparison, the relaxation data of bulk ethylene glycol is given as well.

the low-frequency loss tail a and the high-frequency loss tail $-ab$, are determined by the underlying distribution in relaxation times. The second term in eq 3 accounts for pure Ohmic conduction.

Alternatively, we have fitted the derivative-based loss spectra $\epsilon''_{deriv}(\omega)$ to the analytical derivative of the Havriliak−Negami function $\partial\epsilon'_{HN}/\partial \ln \omega$:

$$\frac{\partial\epsilon'_{HN}}{\partial \ln \omega} = -\frac{ab\Delta\epsilon(\omega\tau)^a \cos[a\pi/2 - (1+b)\theta_{HN}]}{[1 + 2(\omega\tau)^a \cos(\pi a/2) + (\omega\tau)^{2a}]^{(1+b)/2}} \quad (4)$$

with

$$\theta_{HN} = \arctan[\sin(\pi a/2)/((\omega\tau)^{-a} + \cos(\pi a/2))] \quad (5)$$

In particular, we have used the fit function $\partial\epsilon'_{HN}/\partial \ln \omega$ in order to find reliable (start) parameters for the two HN functions (1st term of eq 3) in cases where the loss ϵ'' did not reveal any peak or shoulder of the slow relaxation process due to dominating Ohmic conduction. In these cases, the fit of $\epsilon''_{deriv}(\omega)$ yielded a first (good) approximation of the HN parameters, which were then used as start parameters for a subsequent fit of the original $\epsilon''(\omega)$ spectra resulting in "refined" fit parameters.

The relaxation times obtained by the HN fit procedures are presented in a relaxation map (Figure 3) and have been fitted with the VFT equation. One clearly sees that indeed most of the relaxation processes show a curvature according to the VFT law as a characteristic feature of cooperative α relaxation processes. The VFT parameters are summarized in Table 1.

Effect of Annealing on the Glass Transitions and Relaxation Strengths. A first impression of the influence of annealing on the dynamic properties of AP/EG mixtures can be obtained by comparing Figures 1 and 2, which show the two relaxation processes α_{EG} and α_{AP} for the two extreme cases of a freshly prepared sample (Figure 1) and a sample (2) that was stepwise annealed up to 120 °C (Figure 2). Although both relaxation processes are still present after annealing, in particular the loss peak of amylopectin undergoes a dramatic upshift by 50−80 °C, depending on the frequency.

To elucidate the role of the thermal history on the relaxation properties, a series of stepwise annealing experiments on three different samples was performed (cf. Table 1). For a fair comparison of the dielectric results we have presented both the loss ϵ''_{deriv} ($f = 14$ Hz) and the dielectric constant ϵ' ($f = 28$ kHz) as a function of the temperature for all eight cooling runs (Figures 3 and 4).

The first two cooling runs were made on sample 1, one immediately after preparation (25 °C), the second after subsequent annealing at 40 °C for 400 min. According to Figures 3 and 4, this treatment already causes a slight shift of the α_{EG} peak accompanied by a strong increase in the α_{AP} peak temperature by approximately 40 °C.

A second fresh sample was treated as follows: annealing at 60 °C for 400 min, measurement during cooling to −120 °C, annealing at 80 °C for 300 min, again cooled and measured, and finally stored at room temperature for 1 week under dry conditions in a desiccator. After this period the sample was further annealed at 100 °C for 300 min, measured upon cooling to −120 °C, and subsequently subjected to 120 °C for 300 min and again measured during cooling.

In contrast to the first annealing step (at 40 °C), the treatments at 60 and 80 °C only result in marginal shifts of the peak positions of both the α_{EG} and the α_{AP} relaxation. Concurrently, the relaxation strengths $\Delta\epsilon$ of both processes decrease by a factor of 2 as can be seen in Figure 4 ($\Delta\epsilon \sim \epsilon''$ peak maximum) or in Figure 5 ($\Delta\epsilon_{EG}$ given by the step in ϵ'). A plausible explanation for the weakening of the α_{EG} peak process is the reduction of the volume fraction of phase-separated EG by diffusion into the molecularly mixed AP/EG phase. On the other hand, the reduction of the α_{AP} relaxation strength is not obvious with

SCHEME 1: Cluster Model of Amylopectin[30]

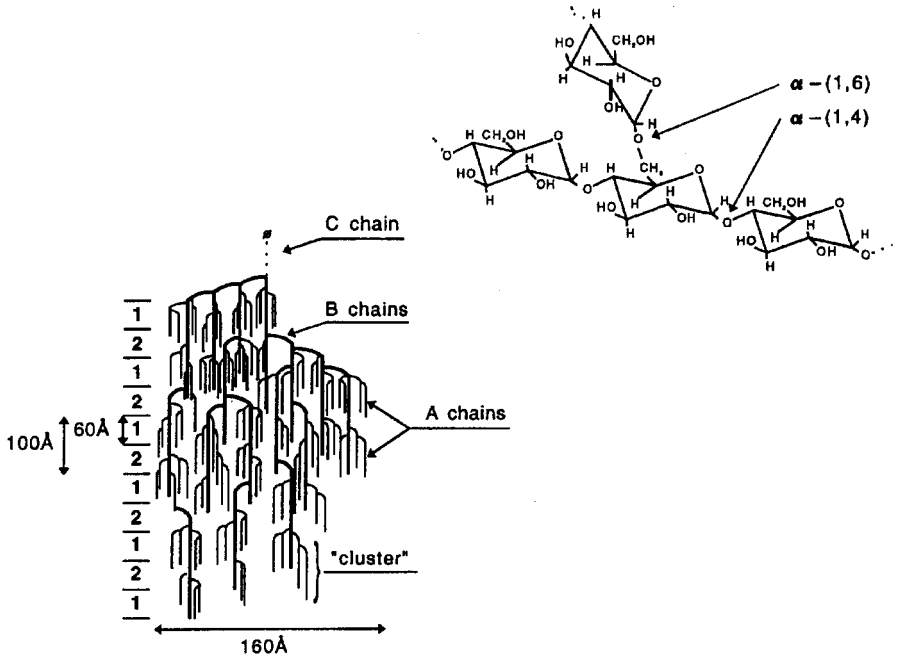

respect to a virtually unchanged glass transition temperature of AP (cf. Figure 3 and the Arrhenius presentation in Figure 5). Most likely, to some extent short-range ordering (e.g., helix formation) or crystallization of AP/EG took place at 60 and 80 °C, temperatures far above (∼100 °C) the estimated glass transition temperature of AP. Explicit evidence for such slow crystallization requires additional studies.

Continued annealing at 100 and 120 °C leads to a further reduction of the free ethylene glycol fraction to about 20% of its initial value, which is again accompanied by a significant increase of the glass transition temperature T_g(AP). Obviously, high-temperature annealing results in an almost complete incorporation of EG in a semicrystalline structure consisting of branched amylopectin macromolecules (see Scheme 1) and H-bonded low-molecular ethylene glycol. Although the details of the molecular organization of such a structure, like the conformation of AP or preferential H-bonding sites, are not known yet, it is obvious that the formation and optimization of the AP/EG structure is a time-consuming process.

An important question is the validity of the time−temperature equivalence for the structure formation which typically holds for thermally activated processes or the glass transition of simple systems. To check this equivalence we tried a different route to obtain a fully cured sample by starting annealing experiments directly at 100 and 120 °C with another freshly prepared sample 3. Interestingly, the dielectric results of sample 3 measured after annealing at 100 and 120 °C strongly resemble those of sample 2 measured at 80 and 100 °C. This "delaying" behavior is plausible due to the shorter thermal/time history of sample 3 and supports the validity of the time−temperature equivalence. However, comparison of the 80 °C curve with the 100 °C (II) curve in Figures 3 and 4, shows that almost identical α_{EG} peak positions and intensities correspond to markedly different intensities of the α_{AP} relaxation. We suggest that the higher α_{AP} relaxation strength of sample 3 can be attributed to a lower degree of short-range order or crystallinity in the AP/EG phase, which points to a melting temperature of helices or AP/EG crystallites between 80 and 100 °C.

So far we have not specified the nature of H-bonding of EG to AP chains in annealed AP/EG mixtures. In principle, the increase in the glass transition temperature of AP by more than 50 °C can be rationalized by different ways of hydrogen bond formation between AP chains and EG molecules. The two main options are chain stiffening by single or double hydrogen bonding of EG molecules or the formation of a physical network by *interchain* EG bridges. Explicit evidence for the existence or nonexistence of *intermolecular* physical cross-links can be obtained from the temperature dependence of the relaxation time of the α_{AP} process, which is shown in Figure 3 and quantified by the VFT fit parameters listed in Table 1.

Compared to the VFT curves of the α_{EG} process at 40 and 60 °C, the α_{AP} relaxation time shows only slightly curved VFT lines, i.e., the α_{AP} process resembles a simple Arrhenius behavior. The degree of curvature of the VFT dependence has been proposed by Angell as a powerful criterion to classify low molecular and polymeric glass formers into fragile glasses (high curvature) and strong glass formers (weak curvature of VFT curve).[21] For polymers, fragility, which can be defined in various ways, is a measure of the degree of intermolecular coupling of polymer chains. Factors that contribute to intermolecular coupling are, for example, sterical hindrance by bulky side groups, covalent cross-links, or other specific *interchain* interactions. A useful quantification of fragility is given by the steepness index *m*, which was defined by Böhmer et al.[22]

$$m = \left.\frac{\mathrm{d}\log\langle\tau\rangle}{\mathrm{d}(T_g/T)}\right|_{T=T_g} \tag{6}$$

m is linked to the VFT parameters by eq 7:

$$m = \frac{E_V}{2.303R}\frac{T_g}{(T_g - T_V)^2} \tag{7}$$

Using eq 7. we have calculated *m* for the α_{AP} relaxation and the results are listed in Table 1. According to reference data[23] our *m* values are at the lower limit, which qualify AP/EG as a very strong glass former, corresponding to a low degree of

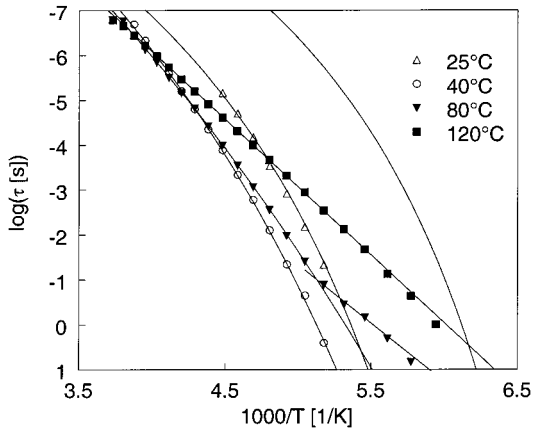

Figure 6. Relaxation time τ_α of the fast α process (α_{EG}) in AP/EG after different thermal treatments. For comparison, the relaxation data of bulk ethylene glycol are shown as a line on the far right.

interchain coupling. Upon annealing, this coupling merely decreases, which makes the idea of a H-bonded AP network created by intermolecular EG bridges unlikely.

This finding rather favors the assumption of *intrachain* EG bridges. In this way, EG is able to occupy H-bonding sites in the AP chain, which inhibits the formation of interchain H-bonds between different AP branches or molecules.

Molecular Dispersion of Ethylene Glycol: Effects of Confinement and Anchoring on Inner Surfaces. While the α relaxation process of the AP structure continuously slows down with increasing annealing temperature (25−120 °C), the (low-temperature) α process of the EG phase shows a more complex behavior (cf. Figure 6). At low annealing temperatures (40 and 60 °C), an initial slowing down of the α_{EG} dynamics can be observed. Heat treatment at higher temperatures then causes a qualitative change of the relaxation time−temperature characteristics from initially VFT behavior to a genuine Arrhenius behavior (100 and 120 °C), which is accompanied by an acceleration of the α process.

This discontinuous shift of the α relaxation time with aging is qualitatively in line with results from EG and other glass forming liquids that are confined to small (nanometers) pores or cages.[24,25] The molecular dynamics of such confined systems is determined by the balance between surface and confinement effects: while interactions with the inner surfaces will delay the molecular dynamics, the reduction in pore size (increase of confinement) will speed up the glass-transition dynamics. In this sense, the initial slow down of the α_{EG} relaxation process in the AP/EG system compared to bulk EG points to a larger amount of less mobile EG located near the inner surfaces of EG droplets after annealing. However, the drastic difference in the dynamics between bulk EG and dispersed EG by 2−3 decades cannot be explained by surface anchoring alone, in particular not in the initial coarse morphology (cf. Figure 9a). We therefore hypothesize that the overall delay of the EG dynamics in AP/EG hints to the existence of a dispersed phase constituted by EG with partially dissolved AP molecules and chain sequences. Such a dilute solution of AP in EG provides a natural explanation for the delayed glass transition of EG without loosing its cooperativity for establishing the VFT dynamics of a bulk liquid.

After annealing at 80 °C, the $\tau(T)$ dependence (Figure 6) becomes flatter and shows a clear deviation from its VFT behavior at lower frequencies. This change in dynamics marks the point at which the size (geometrical confinement) of the glass forming molecular ensemble starts to influence its

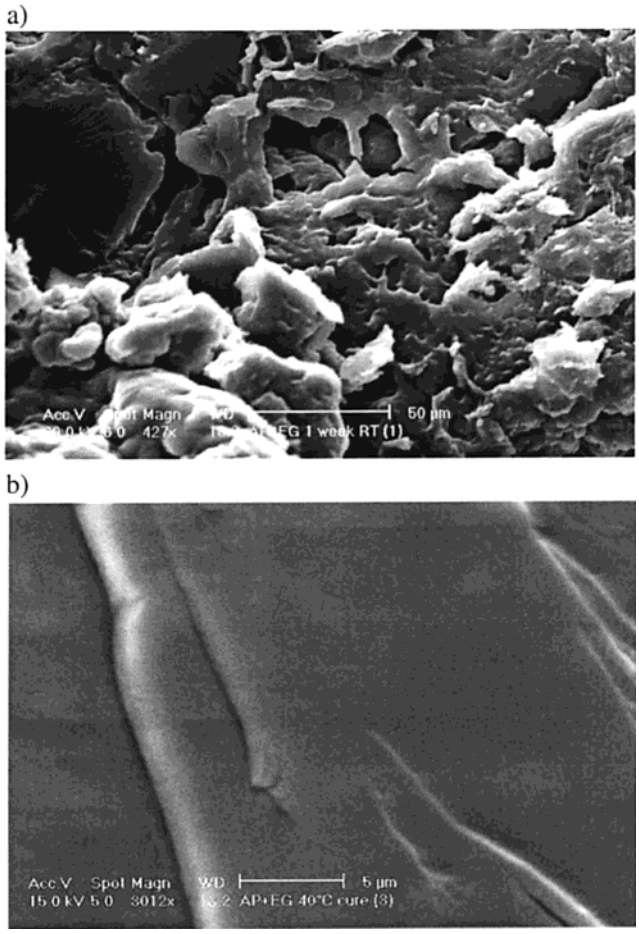

Figure 7. SEM photographs of two AP/EG samples with different thermal histories: (a) after storage at room temperature for 1 week and (b) after 40 °C annealing and subsequent storage at room temperature for 4 weeks.

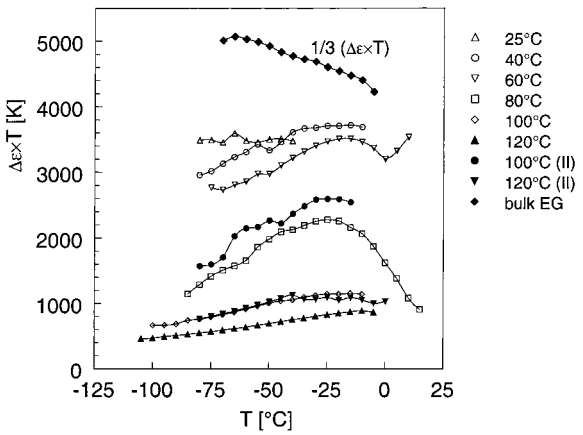

Figure 8. Relaxation strength $\Delta\epsilon$ times temperature T vs temperature T for the α_{EG} process in bulk EG and in AP/EG after different thermal treatments. For an easier comparison, the $\Delta\epsilon T$ data for bulk EG have been reduced to one-third of their original values.

cooperative dynamics. Whereas in the bulk the characteristic length of cooperativity ξ increases with decreasing temperature leading to a curved VFT dependence, one intuitively expects a qualitative change of the $\tau(T)$ dependence in the case that ξ becomes restricted by the geometrical limits of the molecular ensemble. Hence, the departure of $\tau(T)$ from a VFT curve implies that the droplet size after annealing at 80 °C has reached the length of cooperativity, which is typically 2−3 nm near the glass transition temperature.[26] Further annealing at 100 and 120

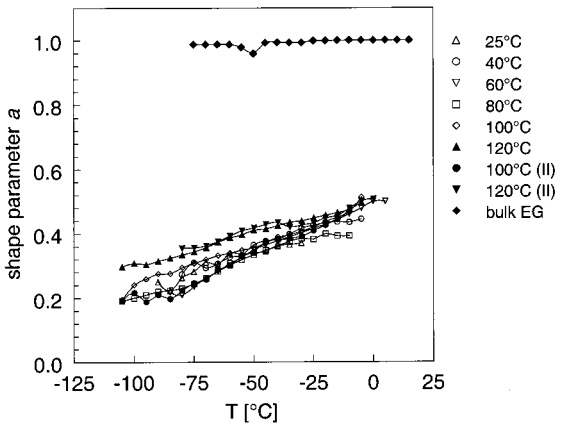

Figure 9. Shape parameter a_{HN} vs temperature for the α_{EG} process in bulk EG and in AP/EG after different thermal treatments.

°C completely alters the dynamics from VFT to a genuine Arrhenius behavior, even for short relaxation times (Figures 3 and 6). In other words, the dynamics of EG has changed from cooperative liquid dynamics to thermally activated, single molecule dynamics. Such a behavior has been previously reported for ethylene glycol that was confined to a variety of zeolitic host systems characterized by different sizes of their pores or cages.[25]

Additional evidence for our molecular picture comes from the relaxation strength $\Delta\epsilon$ and the shape parameter a_{HN} of the α_{EG} relaxation process. Figure 8 displays the temperature dependence of the quantity $\Delta\epsilon T$ for bulk EG as well as for all the AP/EG samples with different thermal history (cf. Table 1). Besides the gradual decrease of the (average) relaxation strength with increasing annealing temperature, a marked change in the temperature dependence of $\Delta\epsilon T$, viz., from a *decrease* (for bulk EG) to an *increase* with increasing temperature can be recognized. While the decrease in $\Delta\epsilon T$ with increasing T is a known property of glass forming liquids, due to gradual loss in cooperativity of the α relaxation,[27] the opposite behavior is usually found for secondary relaxations and other thermally activated relaxation processes.[28] Consequently, the qualitative change in the slope $d(\Delta\epsilon T)/dT$, according to Figure 8, is in agreement with the change from VFT to Arrhenius behavior, caused by increased confinement of the dispersed EG phase.

In contrast to the relaxation strength, the shape of the loss peak of the α_{EG} process is quite different between AP/EG samples and bulk EG. This is expressed by the shape parameter a_{HN}, describing the low-frequency slope of the spectra $\log(\epsilon'')$ vs $\log(f)$ (cf. Figure 9). However, a_{HN} appears to be insensitive to the thermal history and thus the morphology of the AP/EG samples. Obviously, the degree of confinement, as manifested in the mean relaxation times $\tau(T)$ (cf. Figures 5 and 6), plays a minor role in the broadening of the α_{EG} peak. Therefore, it is suggested that the tremendous broadening reflects the (bulk) dynamics of the dispersed EG fraction modified by dissolved AP molecules or chain segments, rather than the influence of surface anchoring of EG molecules as studied by other authors.[29]

The reduction of the final droplet size to far below the μm-range was also clear from the optical appearance of the AP/EG samples, which changed from white (light scattering) to transparent upon annealing. This finding was corroborated by results from scanning electron microscopy (SEM) experiments, shown in Figure 7a,b. Whereas a microporous morphology with a characteristic size of a few μm remains present after short storage at room temperature, no structural details could be detected anymore in a sample that was exposed to 40 °C and subsequently stored for 4 weeks. Breaking the latter resulted in very smooth fracture surfaces as is demonstrated in Figure 7b. A strong hint that EG is still present in a dispersed phase at a size inaccessible to SEM was noticed by the observation, that higher e-beam radiation power resulted in strong plastic deformation and finally bursting of the heated area, most likely caused by the evaporation of EG.

Conclusions

The structure evolution of amylopectin/ethylene glycol mixtures was studied with dielectric relaxation spectroscopy. Both long-time storage at room temperature and annealing at elevated temperatures provoked a significant rise of the dynamic glass transition (T_g increase) of the initially "plasticized" AP phase. Results from samples with a different thermal history imply the validity of the time−temperature equivalence for structure formation kinetics.

A detailed analysis of the VFT temperature dependence of the relaxation time of the dynamic glass transition process of AP (α_{AP}) indicated that AP/EG mixtures behave like strong glasses, which points to a low degree of dynamic coupling between different AP chains. From this finding we conclude that upon time/temperature treatment chain stiffening and *interchain* decoupling of AP chain segments is promoted by H-bonded EG molecules.

The increase in T_g of AP was accompanied by a continuous reduction of the EG droplet size, resulting in nanometer size droplets in which about 20% of the initial amount of EG concentrates. In such a small geometry ethylene glycol becomes dynamically confined, which results in a transition of the α_{EG} dynamics from VFT toward a genuine Arrhenius behavior. This confinement effect is accompanied by a general delay in the dynamics of dispersed EG, due to interaction of EG molecules with partially dissolved AP chains in the EG rich phase. These results are in agreement with previously reported data on the interaction between starch polysaccharides and glycerol or ethylene glycol, which showed that time as well as heat strongly immobilize the plasticizer.[12,13]

Confinement effects on the glass transition dynamics of EG in polymer dispersed nanodroplets have not been reported previously. Furthermore, the results lead to new insights in the influence of polyols on the molecular organization in starch. Interactions between starch and glycerol, ethylene glycol, or other plasticizers, and especially the formation of a structure preventing *interchain* H-bonding between AP chain segments, reduces starch recrystallization/retrogradation. This may improve the control of the mechanical properties of the products and expand the use of starches for various applications.

Acknowledgment. We would like to thank Stephen Picken for stimulating discussions. Furthermore, we thank ATO and the Delft University of Technology for the use of their facilities as well as the Technology Foundation STW of The Netherlands Organization for Scientific Research (NWO) for their financial support (Project UCH.4952).

References and Notes

(1) Gudmundsson, M. *Thermochim. Acta* **1994**, *246*, 329.
(2) van Soest, J. J. G.; Borger, D. B. *J. Appl. Polym. Sci.* **1997**, *64*, 631.
(3) Tharanathan, R. N. *J. Sci. Ind. Res.* **1995**, *54*, 452.
(4) van Soest, J. J. G.; Hulleman, S. H. D.; de Wit, D.; Vliegenthart, J. F. G. *Carbohydr. Polym.* **1996**, *29*, 225.
(5) Thiewes, H. J.; Steeneken, P. A. M. *Carbohydr. Polym.* **1997**, *32*, 123.

(6) Krog, N.; Oleson, S. K.; Toernaes, H.; Joensson, T. *Cereal Foods World* **1989**, *34*, 281.
(7) Kohyama, K.; Nishimura, K. *J. Agric. Food Chem.* **1991**, *39*, 1406.
(8) Katsuta, K.; Miura, M.; Nishimura, A. *Food Hydrocolloids* **1992**, *6*, 187.
(9) Katsuta, K.; Nishimura, A.; Miura, M. *Food Hydrocolloids* **1992**, *6*, 387.
(10) Bello-Pérez, L. A.; Parades-López, O. *Starch/Stärke* **1995**, *47*, 83.
(11) van Soest, J. J. G.; de Wit, D.; Tournois, H.; Vliegenthart, J. F. G. *Polymer* **1994**, *35*, 4722.
(12) Smits, A. L. M.; Hulleman, S. H. D.; van Soest, J. J. G.; Feil, H.; Vliegenthart, J. F. G. *Polym. Adv. Technol.* **1999**, *10*, 570.
(13) Kruiskamp, P. H.; Smits, A. L. M.; van Soest, J. J. G.; Vliegenthart, J. F. G. *Ind. Microbiol. Biotechnol.* **2001**, *26*, 90.
(14) Ikeda, S.; Kumagai, H.; Nakamura, K. *Carbohydr. Res.* **1997**, *301*, 51.
(15) Montès, H.; Cavaillé, J. Y. *Polymer* **1999**, *40*, 2649.
(16) Butler, M. F.; Cameron, R. E. *Polymer* **2000**, *41*, 2249.
(17) Lourdin, D.; Ring, S. G.; Colonna, P. *Carbohydr. Res.* **1998**, *306*, 551.
(18) Mertens, I. J. A.; Wübbenhorst, M.; Oosterbaan, W. D.; Jenneskens, L. W.; van Turnhout, J. *Macromolecules* **1999**, *32*, 3314−3324.
(19) Wübbenhorst, M.; Van Koten, E.; Jansen, J.; Mijs, W.; van Turnhout, J. *Macromol. Rapid Commun.* **1997**, *18*, 139−147.
(20) Wübbenhorst, M.; van Turnhout, J. *Dielectrics Newsletter*, *Novocontrol GmbH* **2000**, *14*, 1−3.
(21) Angell, C. A. *J. Non-Cryst. Solids* **1985**, *73*, 1.
(22) Böhmer, R.; Ngai, K. L.; Angell, C. A.; Plazek, D. J. *J. Chem. Phys.* **1993**, *99*, 4201.
(23) Richert, R.; Angell, C. A. *J. Chem. Phys.* **1998**, *108*, 9016−9026.
(24) Arndt, M.; Stannarius, R.; Groothues, H.; Hempel, E.; Kremer, F. *Phys. Rev. Lett.* **1997**, *79*, 2077−2080.
(25) Huwe, A.; Kremer, F.; Behrens, P.; Schwieger, W. *Phys. Rev. Lett.* **1999**, *82*, 2338.
(26) Donth, E. *J. Non-Cryst. Solids* **1982**, *53*, 325.
(27) Schönhals, A.; Kremer, F.; Hofmann, A.; Fischer, E. W.; Schlosser, E. *Phys. Rev. Lett.* **1993**, *70*, 3459−3462.
(28) Schlosser, E.; Schönhals, A.; Carius, H. E.; Goering, H. *Macromolecules* **1993**, *26*, 6027−6032.
(29) Gorbatschow, W.; Arndt, M.; Stannarius, R.; Kremer, F. *Europhys. Lett.* **1996**, *35*, 719−724.
(30) Hizukuri, S. *Carbohydr. Res.* **1986**, *147*, 342−347.